Eur. Phys. J. B **57**, 305–312 (2007)
DOI: 10.1140/epjb/e2007-00164-9

THE EUROPEAN PHYSICAL JOURNAL B

Molecular dynamics simulations of thermodynamics, elastic constants and solid solution strengths for Mg-Gd alloys

Y. Wu[a] and W. Hu[b]

Department of Applied Physics, Hunan University, Changsha 410082, P.R. China

Received 28 November 2006 / Received in final form 19 February 2007
Published online 6 June 2007 –

Abstract. The thermal and mechanical properties of Mg-Gd intermetallics MgGd, $MgGd_2$ and $MgGd_3$ are studied using a modified analytical embedded atom method. Calculated results agree well with the available experimental data and other theoretical results. The results on the elastic constants suggest that thermal softening behavior is observed as the temperature increases and the bulk moduli of ordered phases are larger than that of elemental Mg above 300 K. The heat capacities of MgGd, Mg_2Gd and Mg_3Gd are 22.91, 23.04 and 23.09 J mol K^{-1}, respectively, at 300 K. Furthermore, the addition of Gd gives rise to an increase of c/a. With the same content of Gd, the ratio c/a remains unchanged with increasing temperature, whereas this phenomenon does not occur in pure Mg, which indicates that the temperature-independent c/a restrains the occurrence of non-basal slip and twinning. Hence the addition of Gd can enhance the strength of Mg, in good agreement with experimental observation.

PACS. 62.20.Dc Elasticity, elastic constants – 65.40.-b Thermal properties of crystalline solids – 31.15.Ct Semi-empirical and empirical calculations

1 Introduction

Magnesium alloys are attractive as comparatively light structural materials. However, they often show poor strength and creep resistance at elevated temperatures. For wider application, it is important to improve strength and creep resistance at elevated temperatures. It is well known that the addition of rare earth metals can optimize mechanical properties and improve creep resistance of magnesium alloys [1–6]. Recently, it was reported that the addition of Gd is effective for improving strength and creep resistance of magnesium alloys at elevated temperature [1,2,7]. Because Gd is a rather expensive metal, it is reasonable to limit its contents to not more than 10 wt.%, although the highest strength of the Mg-Gd binary alloys takes place at approximately 20 wt.%. When Gd content is 20 wt.%, the density of Mg alloys increases to about 2.05 g cm^{-3}, which is also a limitation. Thus the strength of Mg-Gd alloys is anticipated to be improved by additions of metals such as Y and Nd [1,8].

Thermal, metallographic and X-ray analyses by Manfrinetti [9] have shown that the Gd-Mg phase diagram is characterized by four intermediate compounds, GdMg (CsCl-type), $GdMg_2$($MgCu_2$-type), $GdMg_3$ (BiF_3-type) and $GdMg_5$ ($GdMg_5$-type). The equilibrium solid solubility of Gd in magnesium is relatively high (4.53 at.% or 23.49 wt.%) at 821 K and decreases exponentially, to 0.61 at.% (3.82 wt.%) as the temperature decreases to 573 K.

In the present work, a modified analytical embedded atom model (EAM) [9] with potential parameters of the pure Gd and Mg metals are used as interatomic potential parameters, using molecular dynamics (MD) to investigate the physical properties of ordered Gd-Mg alloys (especially, GdMg (CsCl), $GdMg_2$ (Cu_2Mg), and $GdMg_3$ (BiF_3)) such as lattice parameter, cohesive energy, enthalpy of formation, and heat capacity. To date only a few reports of the elastic constants and the bulk modulus of Mg-Gd intermetallics are available in the literature. So we calculated elastic constant and bulk modulus for Mg-Gd intermetallics at various temperatures. Furthermore, solution-strengthening properties of Mg-Gd alloys were also investigated. The results are compared with the available experimental and theoretical data.

2 Embedded atom method

The basic modified analytical embedded atom method (EAM) equations for hcp metals are given [10] by

$$E_t = \sum_i F_i(\rho_i) + \frac{1}{2}\sum_j \phi(r_{ij}) + M_i(P_i) + N_i(Q_i) \quad (1)$$

[a] e-mail: winwyr@126.com
[b] e-mail: wangyuhu2001cn@yahoo.com.cn

with the host electron density

$$\rho_i = \sum_{j(\neq i)} f(r_{ij}) \tag{2}$$

and the argument of the energy modification term

$$P_i = \sum_{j(\neq i)} f^{12}(r_{ij}) \tag{3}$$

$$Q_i = \sum_{j(\neq i)} f^{21}(r_{ij}). \tag{4}$$

The atomic electron density $f(r_{ij})$ is taken as the same function as used by Johnson [11]

$$f(r_{ij}) = f_e \left(\frac{r_1}{r_{ij}}\right)^{4.5} \left(\frac{r_{ce} - r_{ij}}{r_{ce} - r_1}\right)^2 \tag{5}$$

where f_e is the scaling factor, which is a constant in the specific alloys. $f(r)$ is truncated at $r_{ce} = r_8 + k_c(r_9 - r_8)$, where r_8 and r_9 are the 8th and 9th nearest neighbor distance for a perfect hcp crystal with its actual c/a ratio, respectively. $f(r)$ is 0 if r is larger than r_{ce}.

The embedding function $F(\rho_i)$ is taken as the universal form by Johnson [11]

$$F(\rho_i) = -F_0 \left[1 - n \ln\left(\frac{\rho_i}{\rho_e}\right)\right] \left(\frac{\rho_i}{\rho_e}\right)^n \tag{6}$$

where F_0 is a constant, ρ_e takes its equilibrium value. n is an adjustable parameter.

The hcp metal pair potential is taken as

$$\phi(r_{ij}) = \sum_{m=-1}^{6} k_m \left(\frac{r_{ij}}{r_1}\right)^m. \tag{7}$$

The atomic interactions is truncated at a specific cutoff distance $r_c = r_7 + k_c(r_8 - r_7)$. k_c is a adjustable parameter, which ensures no oscillation in the pair potential and the crystal stability.

The energy modification term is empirically taken as

$$M(P_i) = \frac{\alpha}{4} \frac{(P - P_e)^2}{(P + P_e)^2} \tag{8}$$

$$N(Q_i) = \frac{\beta}{4} \frac{(Q - Q_e)^2}{(Q + Q_e)^2} \tag{9}$$

where P_e and Q_e are their equilibrium values.

The Gd-Mg alloy potential is taken as

$$\phi^{ab}(r) = \frac{1}{2}\left[\frac{\chi^b r^b}{\chi^a r^a}\phi^a\left(r\frac{r^a}{r^c}\right) + \frac{\chi^a r^a}{\chi^b r^b}\phi^b\left(r\frac{r^b}{r^c}\right)\right] - \mu\left|\phi^a\left(r\frac{r^a}{r^c}\right) - \phi^b\left(r\frac{r^b}{r^c}\right)\right| \tag{10}$$

where the superscripts a, b indicate atom a-, b- respectively. $\phi^a(r)$ and $\phi^b(r)$ are the monatomic potentials which could be given by the monatomic models. χ is chemical scale. r^a and r^b are a- and b-type atoms parameter, respectively, r^c and μ are alloy adjustable parameters, 3.3773 Å and 0.01, respectively. The above Gd and Mg parameters are given in Tables 1, 2.

3 Simulation details

The physical properties for Gd-Mg ordered alloys are simulated using molecular dynamics. The equations of motion are solved using a fourth-order predictor-corrector algorithm of Gear with a time step of 3×10^{-15} s [12]. The simulations are carried out in two ensembles successively. Some thermal properties such as lattice constant, cohesive energy, enthalpy of formation and density are determined from the constant temperature-constant pressure (NPT) ensemble simulations. Finally, the constant volume-constant temperature (NVT) ensemble is used to compute the elastic constants, heat capacity, free energy and vibrational entropy. The simulation boxes for GdMg, $GdMg_2$, and $GdMg_3$ intermetallic compound system are $10a \times 10a \times 10a \times 2 = 2000$ $6a \times 6a \times 6a \times 16 = 3456$, and $6a \times 6a \times 6a \times 24 = 5184$ particles, respectively.

The fluctuation formula for the calculation of the elastic constants [13,14] is given as

$$C_{\alpha\beta\gamma\kappa} = \frac{\Omega_0}{k_B T}\left(\langle P_{\alpha\beta}P_{\gamma\kappa}\rangle - \langle P_{\alpha\beta}\rangle\langle P_{\gamma\kappa}\rangle\right) + \frac{2Nk_BT}{\Omega_0}\left(\delta_{\alpha\gamma}\delta_{\beta\kappa} + \delta_{\alpha\kappa}\delta_{\beta\gamma}\right) + \langle\chi_{\alpha\beta\gamma\kappa}\rangle \tag{11}$$

where $\langle\rangle$ denotes the averaging over time and Ω_0 is the reference volume for the model system. The first term represents the contribution of the fluctuation of the microscopic stress tensor, $P_{\alpha\beta}$, the second term is the kinetic energy contribution and the third term represents the contribution of the Born term to the elastic constant. The bulk modulus could be obtained from $B = (C_{11} + 2C_{12})/3$ for a cubic lattice.

In addition, in order to compare with EAM calculations, the calculations employed density functional theory under the local density approximation (LDA) embodied in the Vienna ab initio simulation package (VASP) [15]. Exchange and correlation energies are treated using the generalized gradient approximations (GGA) by Perdew and Wang (PW91) [16]. Projector augmented wave (PAW) functions [17] are used. The energy cut-off is chosen to be 400 eV. Brillouin-zone integrations were performed using Monkhorst and Pack [18] k-point meshes, the k-meshes for MgGd (CsCl), Mg_2Gd (Cu_2Mg) and Mg_3Gd (BiF_3) structures are $11 \times 11 \times 11$, $9 \times 9 \times 9$ and $9 \times 9 \times 9$, respectively.

4 Results and discussion

4.1 Lattice parameter, energy and volume thermal expansion

Table 3 shows the results of the cohesive energy and the equilibrium lattice constants for various intermetallic phases calculated from the NPT ensemble averaged over 30 000 time steps at various temperatures along with the available experimental data [9] as well as VASP calculations at 0 K. The EAM calculated lattice parameters

Table 1. Parameters of the many-body potentials for Gd and Mg. n, f_e, χ and k_c are dimensionless, F_0, α, and β in eV, $r^p (p = \text{a, b})$ in Å.

	n	F_0	α	β	k_c	r^p	χ	f_e
Gd	0.41	2.556686	−0.006727	−0.0082697	0.58	3.6519	0.6975	0.09
Mg	0.55	0.759298	0.041349	−0.014632	0.10	3.1851	1.2800	0.25

Table 2. Parameters of the many-body potentials for Gd and Mg. k_i $(i = -1, 0, 1, 2, 3, 4, 5, 6)$ in eV.

	k_{-1}	k_0	k_1	k_2	k_3	k_4	k_5	k_6
Gd	240.3793	−1142.5595	2316.513	−2601.5713	1747.357	−701.1007	155.398	−14.6617
Mg	33.19977	−113.80804	144.6182	−75.965385	2.532347	14.24935	−5.65034	0.69368

Table 3. Comparisons of the lattice constant, cohesive energy and density for different intermetallic phases, predicted from NPT ensemble at various temperatures, including the available experimental data [9] as well as VASP results.

T (K)	GdMg (CsCl)		$GdMg_2$ ($MgCu_2$)		$GdMg_3$ (BiF_3)	
	E_c/kJmol^{-1}	a /Å	E_c/kJmol^{-1}	a /Å	E_c/kJmol^{-1}	a /Å
0	−292.75	3.7976,3.811[a]	−250.86	8.5411,8.547[a]	−221.122	7.4020,7.323[a]
100	−291.46	3.8049	−249.60	8.5563	−219.94	7.4179
200	−290.13	3.8130	−248.31	8.5751	−218.69	7.4373
300	−288.76	3.8215,3.820[b]	−247.01	8.5945,8.575[b]	−217.33	7.4560,7.324[b]
400	−287.36	3.8300	−245.70	8.6127	−215.89	7.4750
500	−285.92	3.8387	−244.36	8.6327	−214.42	7.4936
600	−284.50	3.8476	−242.99	8.6526	−212.87	7.5145
700	−282.89	3.8577	−241.62	8.6712	−211.24	7.5362
800	−281.33	3.8676				
900	−279.76	3.8776				

[a] Calculated from VASP; [b] reference [9].

for GdMg, GdMg, $GdMg_2$, and $GdMg_3$ ordered alloys are compared with the experimental and VASP results, which show good agreement, within about 1%. As shown in Table 3, it is noted that the cohesive energy and the lattice constants for each ordered phase increase as the temperature increases.

Experimentally and theoretically, the enthalpies of formation for GdMg, $GdMg_2$, and $GdMg_3$ intermetallics are −17.5, −20.0 and −19.0 kJ mol^{-1} reported by Pahlman [19], and −17.2, −19.8 and −16.0 kJ mol^{-1} calculated by Cacciamani [20], respectively. The present EAM calculated results of GdMg, $GdMg_2$ and $GdMg_3$ are −16.65, −17.13, −12.37 kJ mol^{-1}, respectively, at 300 K. The comparison with experiment [19] and other theoretical data [20] shows a satisfactory agreement for those intermetallics.

The coefficient of thermal volume expansion is calculated as follows

$$\alpha_P = \frac{1}{V(T)} \left(\frac{\partial V(T)}{\partial T} \right)_P . \tag{12}$$

The values of thermal expansion calculated form equation (12) at 300 K for MgGd, $MgGd_2$ and $MgGd_3$ ordered alloy are listed in Table 4, with experimental data [21,22] included. The value of thermal expansion calculation for Gd is in good agreement with the experimental data [21], while the value of Mg is slightly larger than that of experiment [22].

Table 4. Coefficients of thermal expansion for Mg, Gd pure metals and their alloys. Thermal expansion values of the metals along with available experimental data [21,22] at 300 K.

		Mg	Gd	MgGd	$MgGd_2$	$MgGd_3$
$\alpha_P \times 10^{-5}$(K^{-1})	This work	8.80	4.52	6.22	6.18	7.20
	Experiment	7.51	4.65			

4.2 Elastic constant and bulk modulus

In this study, 30 000 steps are employed to relax in NVT ensemble, then elastic constants are calculated using the fluctuation expression (11) by taking the average over 30 000 time steps. At each temperature, 50 000 steps were carried out to achieve equilibrium. The density obtained from the NPT ensemble by averaging over 30 000 time steps is used to specify the volume of the NVT ensemble. The elastic constants and bulk modulus of MgGd, Mg_2Gd, and Mg_3Gd ordered alloys predicted from the present EAM at various temperatures and VASP at 0 K are listed in Table 5, where the VASP calculated elastic constants are described in detail in reference [23]. For MgGd, there is some discrepancy between the EAM and VASP calculations. Additionally, it can be noted that C_{12} is larger than C_{44} from the present EAM, on the contrary, C_{12} is smaller than C_{44} using VASP. For the other ordered alloys, the theoretical or experimental data on elastic constants are not available in the literature. As shown in

Table 5. Elastic constants and bulk modulus of different ordered alloys at various temperatures, calculated from NVT ensemble. Elastic constants and bulk modulus are in units of GPa. Bulk modulus are calculated from the expression of $B = (C_{11} + 2C_{12})/3$ for the cubic systems. The values in the parentheses are the VASP calculations.

Phases	T (K)	C_{11}	C_{12}	C_{44}	B
GdMg	0	85.51(55.09)	59.22(35.84)	21.20(42.02)	67.98(42.26)
	100	67.78	48.12	40.87	54.67
	300	60.95	45.47	37.61	50.63
	400	58.63	43.62	36.03	48.62
	500	56.72	41.77	34.51	46.75
	600	55.11	40.17	33.21	45.15
	700	53.51	38.38	31.72	43.42
	800	52.16	37.53	30.50	42.41
	900	51.11	36.32	29.23	41.25
$GdMg_2$	0	61.52	29.11	24.57	39.91
	100	53.60	27.59	22.16	36.26
	200	53.43	26.85	21.12	35.71
	300	53.34	26.50	20.10	35.45
	400	53.16	26.42	20.00	35.33
	500	52.72	26.33	19.85	35.13
	600	52.22	26.12	19.70	34.82
	700	51.19	25.91	19.57	34.34
$GdMg_3$	0	70.58	57.67	47.50	61.97
	100	59.48	49.24	37.06	52.65
	200	55.92	46.38	36.51	49.56
	300	52.41	43.38	34.85	46.39
	400	49.88	40.84	33.08	43.85
	500	48.16	38.76	31.48	41.89
	600	46.68	36.80	29.89	40.09

Table 5, elastic constants decrease as temperature increases, indicating thermal softening of the alloy.

In Table 6, the contributions of kinetic-energy, fluctuation and Born terms to elastic constants for MgGd are tabulated separately to show the respective weights of these terms in the simulation results. The corresponding weights of these terms for other ordered alloys are similar to that of B2-MgGd. The largest contribution comes from the Born term to elastic constants as shown in Table 6. The fluctuation contribution is negative for all elastic constants. Fluctuation contribution increases with temperature. This is due to a broader distribution of the microscopic stress tensor. The kinetic energy terms are small (1–2%) for all elastic constants at various temperatures, but they increase with temperature except for all C_{12}. The kinetic energy terms of all C_{12} are zero because of the Kronecker delta in equation (11).

The temperature dependence of bulk moduli of ordered phases and pure metals Mg and Gd is shown in Figure 1, as well as available experimental data [24,25]. The bulk modulus of Mg_2Gd varied slightly with increasing temperature, whereas that of MgGd and Mg_3Gd varied sharply. Above 300 K, the bulk modulus of ordered phases are larger than that of elemental Mg, which indicates that those ordered phases may be strengthening phases in Mg-Gd system. In fact, there are other strengthening mechanism in Mg-Gd system, such as solution-hardening and precipitation-hardening, as reported in experiments [1,26].

The above calculated elastic constant results for Mg-Gd alloys show that the crystals are elastically stable since the stability conditions $C_{44} > 0$, $C_{11} > 0$, and $C_{11} > C_{12}$ are satisfied and thermal softening behavior is observed as the temperature increases.

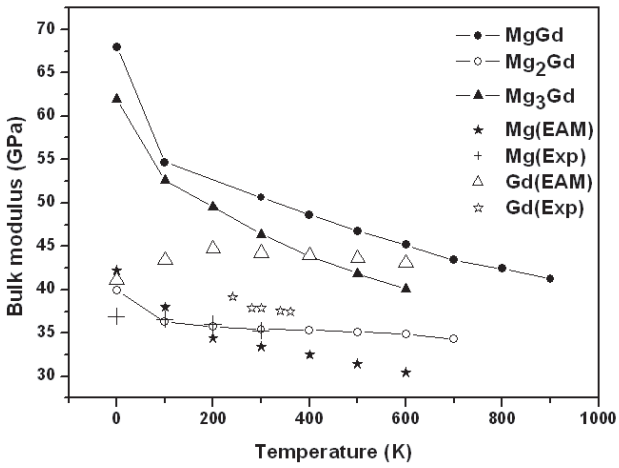

Fig. 1. The temperature dependence of bulk modulus for ordered phases and pure metals Mg and Gd, along with the available experimental data [24,25].

4.3 Vibrational density of states and heat capacity

In this section, we focus our attention on the thermodynamic properties. The velocity autocorrelation function is

Table 6. The contributions to elastic constants of MgGd intermetallic alloy due to the Born, Fluctuation and Kinetic energy terms for the present EAM calculations. The units are in GPa.

T/K		Born term	Fluctuation term	Kinetic energy	Total
300	C_{11}	70.61	−10.25	0.59	60.95
	C_{12}	52.46	−6.99	0.00	45.47
	C_{44}	44.69	−7.38	0.30	37.61
400	C_{11}	68.20	−10.36	0.79	58.63
	C_{12}	50.74	−7.12	0.00	43.62
	C_{44}	43.00	−7.36	0.39	36.03
500	C_{11}	66.33	−10.59	0.98	56.72
	C_{12}	49.07	−7.30	0.00	41.77
	C_{44}	41.43	−7.41	0.49	34.51
600	C_{11}	64.59	−10.64	1.16	55.11
	C_{12}	47.56	−7.39	0.00	40.17
	C_{44}	39.94	−7.31	0.58	33.21
700	C_{11}	62.94	−10.78	1.35	53.51
	C_{12}	45.91	−7.53	0.00	38.38
	C_{44}	38.35	−7.30	0.67	31.72

$Z_\alpha(t)$ defined as

$$Z_\alpha(t) = \frac{\langle v_{i\alpha}(0) v_{i\alpha}(t)\rangle}{\langle v_{i\alpha}(0)^2\rangle} \tag{13}$$

where $v_{i\alpha}(t)$ is the velocity of particle i of type α at time t and $\langle\rangle$ denotes an ensemble average as well as average over all particles of type α. The vibrational density of states $G_\alpha(\omega)$ is obtained from the Fourier transform of the velocity-velocity correlation function

$$G_\alpha(\omega) = \frac{6N_\alpha}{\pi}\int_0^\infty Z_\alpha(t)\cos(\omega t)dt. \tag{14}$$

There are several approaches to the calculation of free energies, constant volume heat capacity and vibrational entropies of solids. A common approach is via the vibrational density of states of the solids. In the harmonic approximation the free energy (F) per atom, constant volume heat capacity per atom and vibrational entropy (S) per atom of a crystal lattice [27] is given by,

$$F = 3k_BT\int d\omega \ln\{2\sinh[\hbar\omega/(2k_BT)]\}G(\omega) \tag{15}$$

$$C_v = 3k_B\int d\omega\left(\frac{\hbar\omega}{2k_BT}\right)^2\left\{\sinh^2[\hbar\omega/(2k_BT)]\right\}^{-1}G(\omega) \tag{16}$$

$$S = 3k_B\int d\omega\left(\frac{\hbar\omega}{2k_BT}\coth[\hbar\omega/(2k_BT] - \ln\{2\sinh[\hbar\omega/(2k_BT)]\}\right)G(\omega) \tag{17}$$

where k_B is Boltzmann's constant and $\hbar$ is reduced Planck's constant. Thus, once the vibrational density of states of a crystal lattice is calculated, one can easily determine its vibrational free energy, heat capacity and vibrational entropy.

The vibrational density of states (VDOS) for MgGd, Mg_2Gd and Mg_3Gd ordered alloys at various temperatures are given in Figure 2. The VDOS for each alloy is normalized to 1. The space group of ordered alloys MgGd, Mg_2Gd and Mg_3Gd is $Pm\bar{3}m$, $Fd\bar{3}m$ and $Fm\bar{3}m$, respectively. The features of the VDOS are more complex as the symmetry decreases and the number of atoms per cell increases. Figure 2 represents those properties. For the same ordered alloy, the VDOS shifts to low frequency with increasing temperature. Figure 3 gives the partial VDOS of MgGd at 300 K. The partial VDOS of other alloys is similar to that of the MgGd ordered alloy. As shown in Figure 3, the VDOS at low frequency originates from the Gd atom, while the VDOS at high frequency comes from the Mg atom, and the contribution of Gd vibrations dominates since it is heavier than Mg.

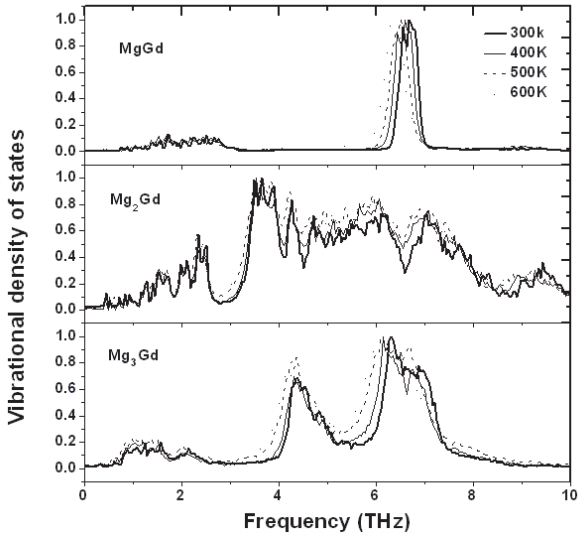

Fig. 2. Vibrational density of states for Mg_xGd_{1-x} compounds at various temperatures.

The heat capacities for MgGd, Mg_2Gd and Mg_3Gd alloys are calculated in this paper at 300 K. Their values are 22.91, 23.04 and 23.09 J mol K^{-1}, respectively.

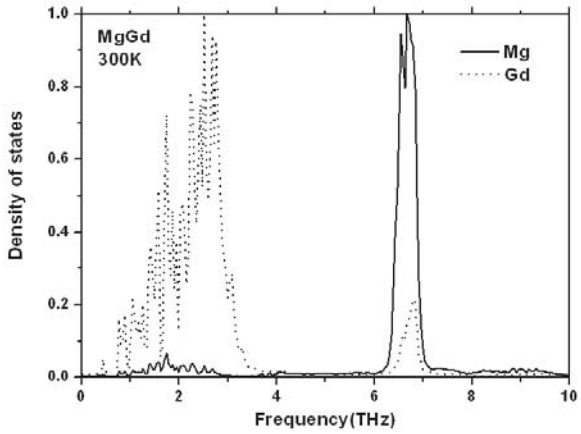

Fig. 3. The partial vibrational density of states for MgGd alloys at 300 K.

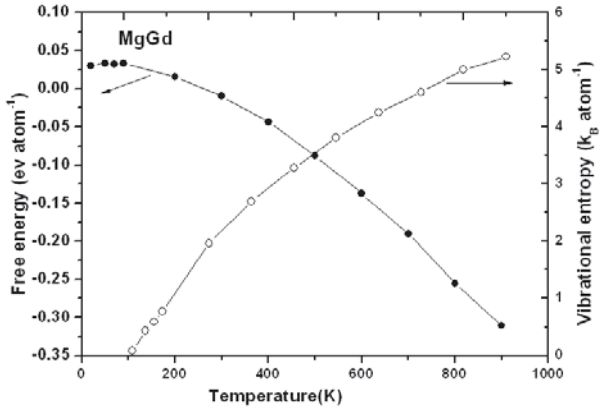

Fig. 4. The temperature dependence of vibrational free energy F and vibrational entropy S for MgGd alloy.

Using the obtained vibrational density of states, $G_\alpha(\omega)$, the free energy and vibrational entropy of MgGd, Mg_2Gd and Mg_3Gd alloy is calculated. The MgGd intermetallic calculated results are plotted in Figure 4, the other intermetallics have the same characteristics. It is clear that the alloy free energy decreases with increasing temperature, while the vibrational entropy of the alloy increases, due to increasing disorder state.

4.4 Effect of Gd on lattice parameters and strength in Mg

Magnesium with hexagonal close-packed crystal structure has three slip systems: a basal slip system of $(0001)\langle 11\bar{2}0\rangle$, a prismatic slip system of $\{10\bar{1}0\}\langle 11\bar{2}0\rangle$ and a pyramidal slip system of $\{10\bar{1}\bar{1}\}\langle 11\bar{2}0\rangle$. The latter two slip systems act together in many cases and are called the non-basal slip system versus the basal slip system. Magnesium is plastically-deformed by the basal slip and twinning mainly at relatively low temperature. The critical resolved shear stress for the basal slip in pure magnesium is very low, approximately 0.6–0.7 MPa, at room temperature, and is independent of temperature. In contrast, the critical shear stress for the non-basal slip is over 40 MPa at low temperature, which is two orders of magnitude higher than that for the basal slip, and drastically decreases to 2–3 MPa with increasing temperature [28].

Experimentally, the equilibrium solid solubility of Gd in magnesium is relatively high (4.53 at.%) at 821 K and decreases exponentially, with a decrease in temperature, to 0.61 at.% at 573 K. It has been reported that the addition of Gd is effective for improving strength and creep resistance of magnesium alloys at elevated temperature [1,2,7]. So in this paper, we simulated effect of Gd on lattice parameter and strength in Mg.

The variation of lattice parameter with temperature in pure Mg and $Mg_{100-x}Gd_x$ ($x = 0.5, 1, 2, 3, 4$ at.%) alloy is shown in Figure 5, along with the experimental data [22]. By adding Gd atoms, the lattice parameters (a, c) and the axis ratio (c/a) become larger, and the a and c in the pure Mg and $Mg_{100-x}Gd_x$ alloy increase linearly with increasing temperature. The EAM calculations are larger than experimental values. As shown in Figure 5c, the c/a in Mg-0.5Gd alloy is constant with temperature, whereas this phenomenon does not occur in pure elemental Mg. Thus, the solid solute Gd gives rise to the variation of lattice parameters, whereas the c/a remains unchanged with increasing temperature, which indicates that the temperature-independent c/a restrains the occurrence of non-basal slip and twinning. The slip and twining in hcp metals can be related to the axis ratio, c/a. Non-basal slip hardly occurs when the c/a is large, whereas at high temperature, where the c/a becomes lower, non-basal slip can occur [29].

As an example of Mg-4Gd, the elastic constants C_{11}, C_{12}, C_{44}, C_{33}, C_{13} are 69.29, 27.47, 14.65, 73.59, 19.91 GPa, respectively, at 300 K. Therefore the solid solubility of Gd in Mg is also elastically stable, in accordance with the stability conditions of hcp crystal, $C_{12} > 0$, $C_{33} > 0$, $C_{44} > 0$, $C_{11} > C_{12}$, and $C_{11}C_{33} + C_{12}C_{33} > 2C_{13}C_{13}$.

The variation of bulk modulus with temperature in pure Mg and $Mg_{100-x}Gd_x$ alloys is presented in Figure 6, along with the experimental data [24]. It can be noted that the addition of Gd gives rise to the increase of bulk modulus of Mg at room and high temperature. This indicates that the addition of Gd can enhance the strength of Mg, in agreement with experiments [1,2,7]. Furthermore, the bulk modulus of Mg increases with increasing the content of Gd.

5 Conclusions

In this paper, we have presented a wide range of properties for ordered alloys MgGd, Mg_2Gd and Mg_3Gd. The temperature dependence of physical properties for MgGd, Mg_2Gd and Mg_3Gd ordered intermetallics are simulated for the first time. The simulated thermal and mechanical properties of Mg-Gd ordered alloys are in good agreement with the available experimental data and the first-principles results. The thermal volume expansion values of

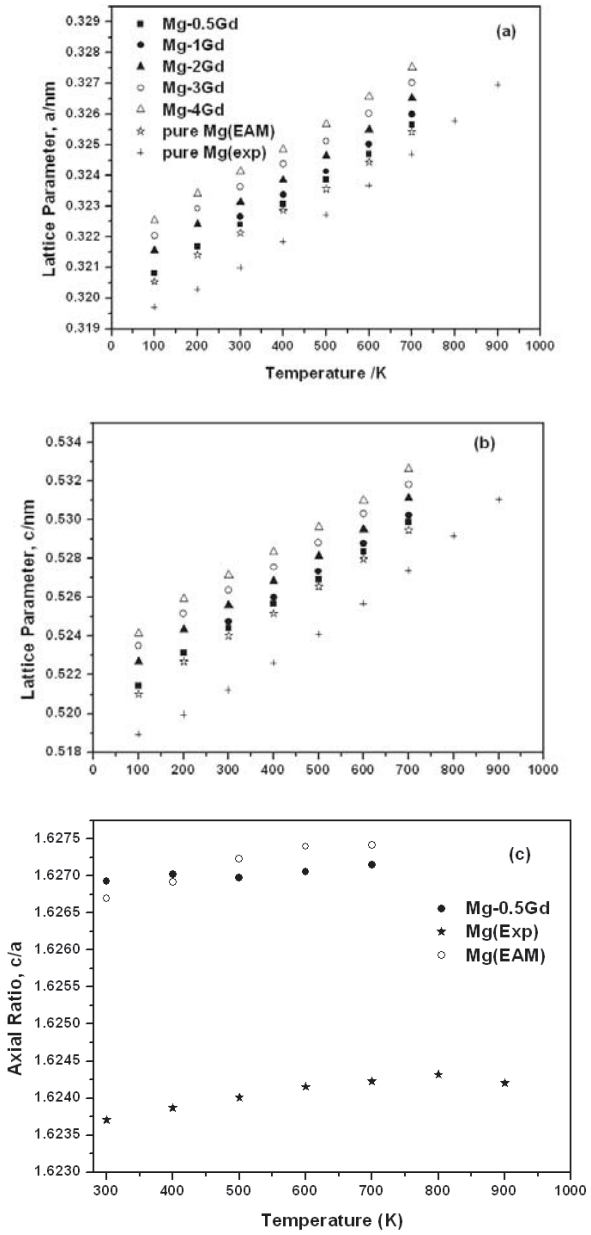

Fig. 5. Lattice parameters a, c, and c/a as a function of temperature for pure Mg, $Mg_{100-x}Gd_x (x = 0.5, 1, 2, 3, 4$ at%) alloys, along with the experimental data [22].

MgGd, Mg_2Gd and Mg_3Gd are 6.22×10^{-5}, 6.18×10^{-5} and 7.20×10^{-5} K^{-1}, respectively, at 300 K. The elastic constant results show that the crystals are elastically stable since the stability conditions $C_{44} > 0$, $C_{11} > 0$, and $C_{11} > C_{12}$ are satisfied and thermal softening behavior is observed as the temperature is increased, and the bulk modulus of ordered phases are larger than that of elemental Mg. Furthermore, the solid solubility of Gd in Mg is also elastically stable, because elastic constants are also accorded with the stability conditions of crystal, $C_{12} > 0$, $C_{33} > 0$, $C_{44} > 0$, $C_{11} > C_{12}$, and

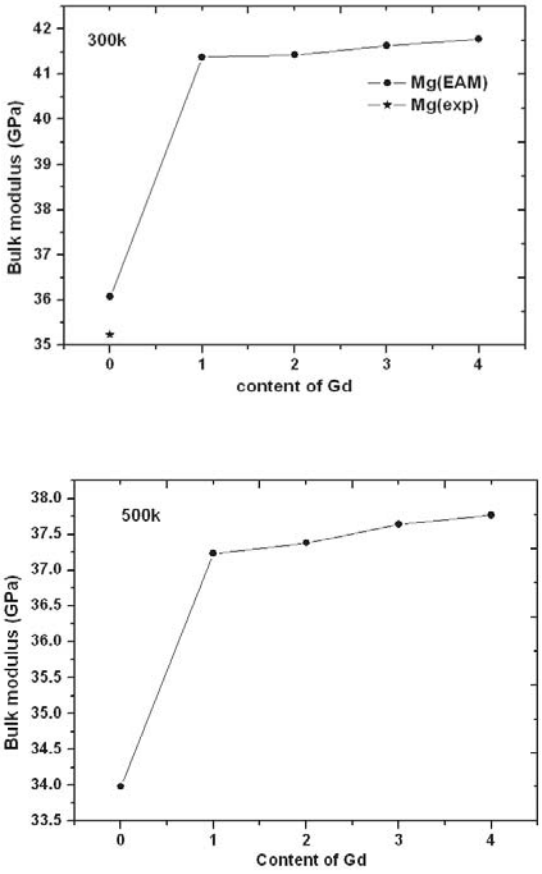

Fig. 6. Bulk modulus of Mg as function of Gd content at room and high temperature, as well as the experimental data [24].

$C_{11}C_{33} + C_{12}C_{33} > 2C_{13}C_{13}$. The addition of Gd gives rise to the increase of c/a at room temperature. The c/a remains unchanged with increasing temperature, whereas this phenomenon cannot be obtained in pure Mg. This indicates that the temperature-independent c/a restrains the occurrence of non-basal slip and twinning. Additionally, Gd increases the bulk modulus of Mg, indicating that addition of Gd can enhance the strength of Mg, which is in good agreement with experiment.

This work is financially supported by the National Natural Science Foundation under contract Nos. 50371026, 50571036 and 50671035.

References

1. L.L. Rokhlin, N.I. Nikitina, Z. Metallkd. **85**, 819 (1994)
2. S.M. He, L.M. Peng, X.Q. Zeng, W.J. Ding, Y.P. Zhu, Mater. Sci. Eng. A **433**, 175 (2006)
3. Mayumi Suzuki, Hiroyuki Sato, Kouichi Maruyama, Hiroshi Oikawa, Mater. Sci. Eng. A **252**, 248 (1998)
4. B.L. Mordike, Mater. Sci. Eng. A **324**, 103 (2002)
5. M. Socjus-Podosek, L. Litynska, Mater. Chem. Phys. **80**, 472 (2003)

6. I.P. Moreno, T.K. Nandy, J.W. Jones, J.E. Allison, T.M. Pollock, Scripta Materialia **48**, 1029 (2003)
7. Peng Qiuming, Wu Yaoming, Fang Daqing, Meng Jian, Wang Limin, J. Rare Earths **24**, 466 (2006)
8. Negishi, Yuuji, Nishimura Takuhiro, Kiryuu Masao, Kamado Shigeharu, Kojima Yo, Ninomiya Ryuuji. Keikinzoku/J. Jap. Inst. Light Metals. **45**, 57 (1995)
9. P. Manfrinetti, K.A. Jr Gschneidner, J. Less-Common Metals **123**, 267 (1986)
10. W. Hu, H. Deng, X. Yuan, M. Fukumoto, Eur. Phys. J. B **34**, 429 (2003)
11. R.A. Johnson, D.J. Oh, J. Mater. Res. **4**, 1195 (1989)
12. M. Parrinello, A. Rahman, J. Appl. Phys. **52**, 7182 (1981)
13. T. Cagin, Ray John R, Phys. Rev. B **38**, 7940 (1988)
14. T.C agin, Ray John R, Phys. Rev. B **37**, 699 (1988)
15. G.Kress, J. Furthmuller, Phys. Rev. B **54**, 11169 (1996)
16. J.P. Perdew, Y. Wang, Phys. Rev. B **45**, 13244 (1992)
17. P.E. Blöchl, Phys. Rev. B **50**, 17953 (1994)
18. M. Methfessel, A.T. Paxton, Phys. Rev. B **40**, 3616 (1989)
19. J.E. Pahlman, J.F. Simth, Metall. Trans. **3**, 2423 (1972)
20. G. Cacciamani, A. Saccone, G. Borzone, S. Delfino, R. Ferro, Thermochimica Acta **199**, 17 (1992)
21. F. Barson, S. Legvold, F.H. Spedding, Phys. Rev. **105**, 418 (1957)
22. Y.S. Touloukian, R.K. Kirby, R.E. Taylor, P.D. Desai, *Thermal Expansion Metallic elements and Alloys*, (IFI/Plenum, New York-Washington, 1977), Vol 12
23. S.Q. Wang, H.Q. Ye, J. Phys.: Condens. Mater **15**, 5307 (2003)
24. L.J. Slutsky, C.W. Garland, Phys. Rev. **107**, 972 (1957)
25. S.B. Palmer, E.W. Lee, M.N. Islam, Proc. R. Soc. Lond. A **338**, 341 (1974)
26. T. Honma, et al., Mater. Sci. Eng. A **395**, 301 (2005)
27. A.A. Maradudin, E.W. Montroll, G.H. Weiss, I.P. Ipatova, *Theory of Lattice Dyanamics in the Harmonic Approximation*, 2nd edn. (New York, 1971)
28. H. Numakura, M. Koiwa, Met. Sci. Tech. **16**, 4 (1998)
29. J.E. Dorn, J.B. Mitchell, *High-Strength Materials* (John Wiley & Sons, Inc. New York, 1964)